THE ASTROPHYSICAL JOURNAL, 412:111–126, 1993 July 20

M82: THE SAGA CONTINUES

K. K. MCLEOD, G. H. RIEKE, M. J. RIEKE, AND D. M. KELLY
Steward Observatory, University of Arizona, Tucson, AZ 85721
Received 1992 September 28; accepted 1993 January 26

ABSTRACT

We present new near-infrared observations of the starburst galaxy M82, including high-resolution J, H, and K imagery, 1–5 μm spectrophotometry and photometry, and 1.05–1.35 μm spectroscopy. These measurements are used to examine the stellar population in the galaxy and conditions in the interstellar medium. We combine our observations with results from the literature to derive a new set of constraints for starburst models, which are presented in a companion paper.

Our measurements of Paschen line fluxes in combination with the strengths of other recombination lines allow study of the reddening in M82. We find that a uniform foreground screen model for the dust geometry cannot explain the relative line strengths. A variety of other models can fit the data reasonably well, such as a nonuniform foreground screen or a homogeneous mix of dust and gas. The derived properties of the galaxy are not strongly dependent on which of these models is selected; we derive an ionizing flux of $\approx 10^{54}$ s^{-1} and an absolute magnitude of the starburst region of $M_K < -22.5$. Depending on the reddening model, the visual extinction to the nucleus lies between $A_V = 12$ and $A_V = 27$; we show that the nucleus does not coincide with any feature that is bright at visual wavelengths. The stellar H_2O index in the nuclear region is less than 0.06 and the CO index is ≈ 0.21; contamination of the CO band by emission by hot dust must be small. We use several lines in the 1.3 μm region to derive a lower limit to the electron density of $n_e > 10^{4.5}$ cm^{-3} in the [Fe II] emission region. The [Fe II] line fluxes are consistent with excitation by fast shocks incident on dense gas. We report the tentative detection of several lines of H_2, which, if confirmed, implicate UV fluorescence as the excitation mechanism.

Subject headings: dust, extinction — galaxies: individual (M82) — galaxies: ISM — galaxies: photometry — galaxies: starburst — infrared: galaxies — ISM: molecules

1. INTRODUCTION

M82 is a unique test laboratory for starburst theories because it appears to have been a relatively low luminosity galaxy prior to the current episode of activity. Since the starburst dominates the preexisting galaxy so strongly, M82 can be approached almost as a "pure" starburst without concern about the contribution from the host galaxy. Furthermore, M82 is exceptionally close so observations can be made on a detailed physical scale. These reasons account for the extensive use of M82 as the archetypical starburst, where theories for this phenomenon are developed and tested.

Strong polarization of light scattered from the filaments originally led to the suggestion that M82 contains an active nucleus (e.g., Lynds & Sandage 1963). However, Solinger, Morrison, & Markert (1977) suggested that M82 was the site of rapid star formation, a hypothesis which was confirmed by the optical spectroscopy of O'Connell & Mangano (1978) and which led to the detailed starburst models of Rieke et al. (1980). The discovery of a complex of supernova remnants lying along the plane of the galaxy (Kronberg, Biermann, & Schwab 1985) confirmed one of the most dramatic predictions of the starburst theory. Recent efforts have concentrated on a more detailed understanding of the physical processes in M82, such as the sequence of star formation within the galaxy, the effects of star formation on the interstellar medium, and the nature of the process of star formation itself.

In this paper, we present new observations of M82 that reveal additional aspects both of its interstellar medium and of its stellar population. These data include high-resolution near-infrared images, spectrophotometry, and spectroscopy. The data help us lay the observational foundation for a new set of starburst models using modern stellar evolutionary tracks (to be presented by Rieke et al. 1993). To achieve this goal, we use our new observations for a critical examination of recent papers, particularly that of Lester et al. (1990, hereafter LCJG). A number of claims in these papers are not confirmed, and the updated observational picture of the galaxy remains generally consistent with that assumed for the starburst models of Rieke et al. (1980).

2. OBSERVATIONS

We report three distinct types of near-infrared observations of M82, which taken together with published data allow us to reexamine the boundary conditions for starburst models and derive new constraints on the conditions in this galaxy. The new measurements are (1) imagery at 1.25, 1.6, and 2.2 μm with angular resolution of $\approx 1''.2$; (2) spectrometry between 1.4 and 3.8 μm at a spectral resolution of $\lambda/\Delta\lambda \approx 80$, with photometry at 5 μm; and (3) spectroscopy between 1 and 1.4 μm at a spectral resolution of $\lambda/\Delta\lambda \approx 800$. Details of the observations are described below.

2.1. *Imagery*

We obtained images of M82 at J (1.25 μm), H (1.6 μm), and K (2.2 μm) on the Steward Observatory 2.3 m telescope on the night of 1990 January 9. The camera used a NICMOS-2 128 × 128 array of HgCdTe detectors; we set the internal optics of the camera to give a nominal scale of $0''.58$ per pixel. We interleaved equal exposures on M82 and on nearby sky for the purpose of flat-fielding. Conditions were photometric, and

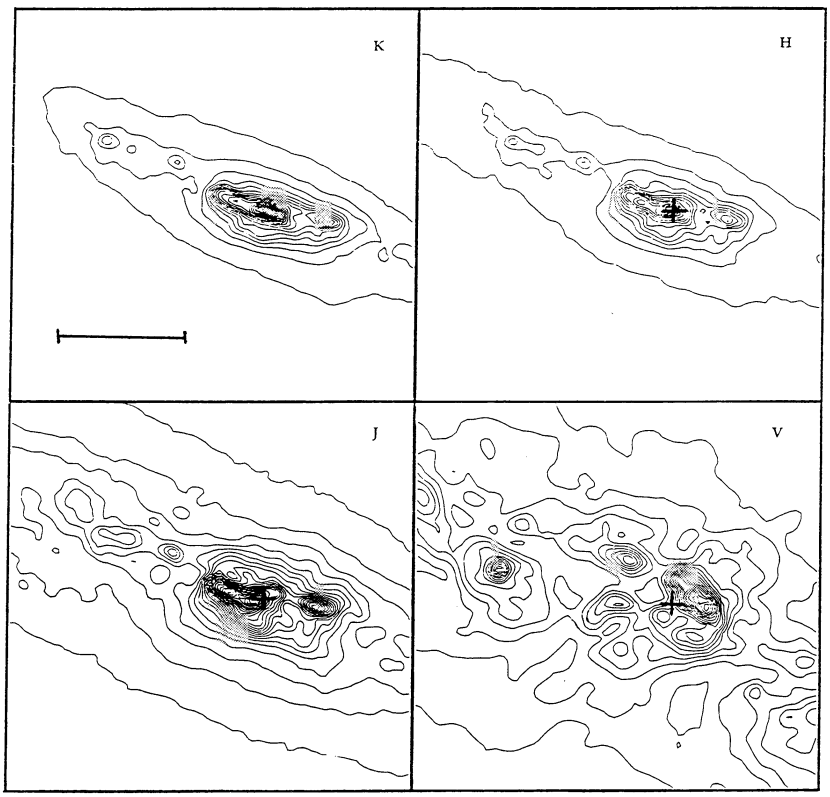

FIG. 1.—Images of M82. The nuclear position at K is marked with a cross on the images at shorter wavelengths. The horizontal bar in the K frame is 10″ = 150 pc in length.

the seeing measured from infrared images of stars was $\leq 1''$ FWHM.

The data were reduced by removing the readout offset, dividing the object frames by the sky frames, renormalizing by the average sky signal, and subtracting a uniform level equal to the average sky. Repeated exposures at the same wavelength were shifted to the same position and averaged. Distances on the frames between field stars and features in M82 were measured to determine the relative plate scales at the three wavelengths, and the images were adjusted to identical scales (the frame at H was magnified by a factor of 1.0096 and that at K by 1.0172). We compared iris photometry of the reduced images with the aperture photometry of Aaronson (1978) to calibrate the frames. The results are shown in Figure 1.

These data appear to be consistent with the frames of Telesco et al. (1991), but with significantly higher resolution resulting from our use of a pixel size of 0.″58 compared with their 1.″35. As a result, small-scale features such as the nucleus of the galaxy are substantially more prominent in our frames.

2.2. *Spectrophotometry*

We obtained spectrophotometry of M82 on 1990 April 9 at the Multiple Mirror Telescope (MMT).[1] The measurements were made with the MMT near-infrared photometer, which uses a single InSb detector operating at liquid helium temperature and a circularly variable filter. The spectral resolution is $\lambda/\Delta\lambda \approx 80$, as determined from measurements of emission lines from astronomical sources. Measurements were made from 1.4 to 3.8 μm through an aperture 5.″4 in diameter and with a chopper throw of 30″. Data points were obtained near the Nyquist sampling spacing (i.e., at roughly two spectral points per spectral resolution element). Observations were made under photometric conditions and scans at all wavelengths were repeated to determine the effects of systematic errors. The errors were found to be less than 3% in all parts of the spectrum (and less than half this value in regions of small atmospheric absorption). Calibration of these scans was obtained through measurements of a variety of solar type stars close to M82 on the sky. The flux for each star was calculated from zero-magnitude fluxes given in Campins, Rieke, & Lebofsky (1985) and the flat-field star's m_V and spectral type.

The observing aperture was placed by pointing the telescope to the reference star BD +70°857 and then using the LCJG offsets (88.″2 E, 111.″8 N) to move to M82's 2 μm nucleus. The MMT's excellent pointing (typically better than half an arcsecond) ensured that our beam was well centered at the LCJG beam center, (1950 $9^h51^m43^s.6 + 69°55'00''$. We then adjusted the telescope position onto the maximum surface brightness at 2.2 μm as measured through this aperture; from inspection of the K image, this position is well centered on the 2 μm nucleus. The corrections to maximize the signal were of the order of 0.″5, within the combined errors of the offsetting and signal peaking. We therefore confirm the position of the infrared nucleus measured by LCJG. Subsequently, the LCJG offsets were used without correction in obtaining the spectrophotometry.

Photometry of the same position, using the same aperture size and chopper throw, was obtained at 3.5 and 4.9 μm using the MMT and the facility bolometer system. This system uses a

[1] The MMT is a joint facility of the Smithsonian Institution and the University of Arizona.

single silicon bolometer operated at a temperature of ≈ 1.1 K. The optical layout is identical to that for the near-infrared photometer. The data were calibrated against the standard star networks discussed by Campins et al. (1985) and Elias et al. (1982). The 4.9 μm photometry was normalized to the spectrophotometry by means of the overlapping data at 3.5 μm.

A second set of measurements was obtained at a position 2″ south and 8″ west of the nucleus of M82 to allow direct comparison with the data of LCJG at this position. The measurement procedures were identical to those described for the nuclear position.

The spectrophotometry and photometry are presented in Figure 2. The two spectra have been set equal at 2.27 μm, just blueward of the CO band head, by multiplying the off-nuclear spectrum by 2.1.

2.3. *Spectroscopy*

The spectra presented here were obtained between 1989 February and 1991 February at the Steward 2.3 m telescope and the MMT. The observations were made with a grating spectrometer that operates between 0.85 and 1.6 μm. The instrument and data reduction techniques are described in Rix et al. (1990). For these measurements, the spectrometer was used with a 600 line mm^{-1} grating that gave a resolution of $\lambda/\Delta\lambda \approx 800$ (determined from the widths of calibration lamp lines). The angular diameter of the circular entrance aperture was 6″ and 3″ respectively on the 2.3 m and MMT. For flat-fielding, several stars of types F3 V to G2 IV were chosen because these types have weak atomic and molecular absorption features. By inspection of the solar spectrum in the vicinity of the Paschen lines, we estimate that the hydrogen absorption lines in the flat-field stars might cause the corresponding M82 emission lines to be overestimated by about 10%.

The resulting MMT spectrum is shown in Figure 3. This spectrum pertains to the nuclear position of M82 as determined by LCJG (see § 2.2 above). The wavelength coverage at a given grating setting is roughly 0.022 μm. To ensure that each piece of the spectrum was sampled at least twice, the MMT observations were made every 0.01 μm between 1.05 and 1.34 μm (with a gap in the region of the 1.14 μm telluric H_2O band).

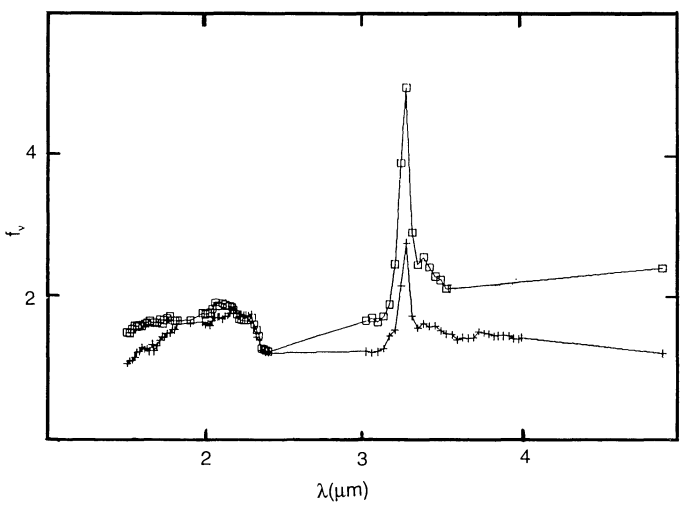

FIG. 2.—Spectrophotometry of M82. Measurements of the nucleus are indicated with pluses and those 8″ W, 2″ S of the nucleus by boxes. The beam was 5″.4 in diameter. The point at 4.9 μm is with a bandwidth of ≈ 0.8 μm; the other data are at a resolution of 80. The spectra have been set equal at 2.27 μm.

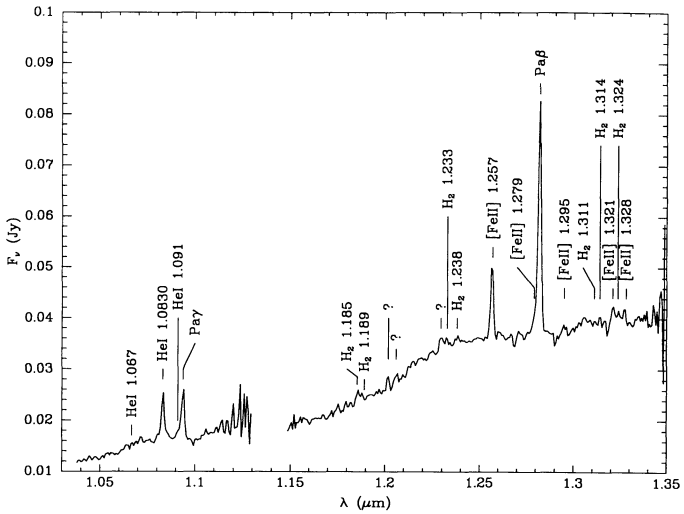

FIG. 3.—Spectrum of the nuclear position of M82, taken at the MMT. The noise in the spectrum near 1.12 and 1.35 μm is due to the poor transmission in the telluric water bands.

Thus the spectrum in Figure 3 is the composite of roughly 30 individual pieces. These pieces were combined using software that compares them in the region of overlap (R. Cutri, private communication). The continuum shape was determined from this composite spectrum. Finally, the spectrum was calibrated against the *J*-band photometry in Rieke et al. (1980), making a small beam size correction from 3″.9 to 3″. The beam size correction was estimated from the growth curve in that paper to be $S_\nu \propto \theta^{5/3}$, where θ is the beam diameter and S_ν is the flux enclosed; thus, the correction was a factor of 0.65.

Data from the 2.3 m also pertain to the *K* nucleus but cover only the wavelengths of Paβ, Paγ, and Paδ. Again, the flux calibration was determined from the Rieke et al. (1980) photometry, with a beam size correction factor of 1.06 to transform from their 5″.8 beam to our 6″ beam.

Line fluxes were determined by fitting Gaussian shapes to the lines using the Levenberg-Marquardt method of finding the minimum of χ^2 and the 1 σ error in each parameter of the fit (Press et al. 1986). In some cases, the lines in question were blended and thus were fitted with multiple Gaussian curves, with the restriction that both components have the same width. The spectra used to get fluxes of the strongest lines are shown in Figure 4. The fluxes quoted in this paper include the 1 σ formal errors from the fitting program; these do not take into account possible systematic errors and uncertainties in the placement of the continuum for each line.

3. DISCUSSION

3.1. *Nuclear Position*

While observing with the spectrophotometer, we found by inspection of the acquisition TV that the 2 μm nucleus of M82 lies behind a lane of heavy obscuration. This observation repeats and confirms a similar one made by Rieke et al. (1980) and demonstrates that knot A (the brightest region of the galaxy optically) is a foreground H II region within M82, not part of the nucleus. The technique employed on both occasions is direct and does not rely on a comparison of coordinates after the fact. The point is reemphasized by the very red color of the nucleus in Figure 1: the nucleus fades into insignificance at 1.25 μm even though it is prominent at 2.2 μm. It therefore is

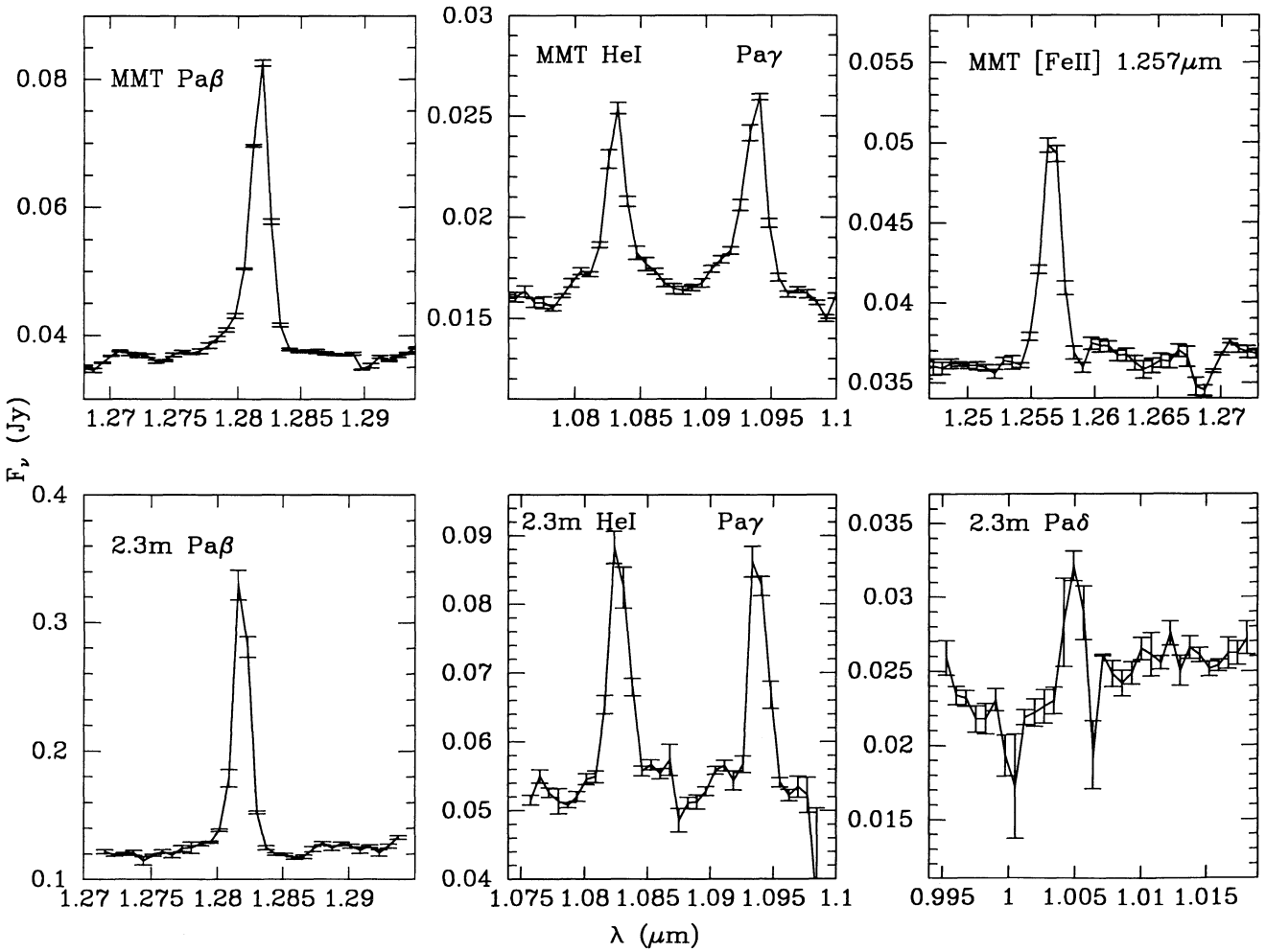

FIG. 4.—Strong emission lines in M82. The beam size at the MMT is 3″, the beam size at the 2.3 m is 6″. Error bars are ±1 σ.

highly unlikely that the 2 μm nucleus is knot A, as suggested by O'Connell (quoted by LCJG).

3.2. H_2O *and* CO *Indices*

Very cool stars have a broad absorption feature at 1.9 μm due to steam. The strength of this feature is often characterized by an H_2O index, which is a measure of the relative signals in two photometric bands, one on continuum at 2.2 μm and the other in the absorption feature at 1.95 μm (see Aaronson, Frogel, & Persson 1978). Our spectrophotometry in Figure 2 shows little evidence for the steam feature. Within our 5″.4 aperture, we obtain an upper limit of 0.06 on the H_2O index (after correcting the spectral slope for extinction). A second prominent absorption in the spectra of cool stars is the (2, 0) band head of CO just longward of 2.29 μm, whose strength is often characterized by another photometric measure, the CO index (see Frogel et al. 1978). Our spectrophotometry yields an estimate of the CO index of 0.20 after correcting the spectral slope for extinction.

Our upper limit for the H_2O index is in good agreement with most previous measurements, from which we have obtained the following limits: (1) ≤0.10 within a 7″.8 aperture (Rieke et al. 1980); (2) ≤0.10 within a 7″.8 aperture (derived from Walker, Lebofsky, & Rieke 1988); and (3) ≤0.07 within a 30″ aperture (Willner et al. 1978). None of these measurements supports the claim by LCJG that the index is ≈0.20 within a 3″.8 aperture. Our new spectrophotometry appears to be in direct contradiction with LCJG since the data were obtained with an aperture of similar size that was carefully centered at the same position on the galaxy. Each of our previous measurements, made with a 7″.8 beam and with two different Fourier transform spectrometers, also appears to disagree with LCJG. Given that at least three different instruments fail to confirm the strong H_2O absorption, we conclude that the measurement of LCJG is likely in error.

Our new estimate of 0.20 for the CO index is very close to the value of 0.22 derived by LCJG and is in exact agreement with the value derived from the Walker et al. (1988) CO equivalent width. The strength of this feature appears to be well measured; we adopt an average value of 0.21. The CO absorption is substantially stronger than the feature observed in the spectra of normal galaxy nuclei, which typically have CO indices of ≈0.15 with relatively little scatter around this value (e.g., Frogel et al. 1978). A detailed comparison that emphasizes this difference is given by Walker et al. (1988). The CO band strength increases with increasing stellar luminosity,

decreasing temperature, and increasing metallicity. Rieke et al. (1993) will examine the cause of the strong CO index in M82. Here we simply note that since dwarf galaxies are generally metal-poor, we would expect M82's CO absorption to be weaker than in normal, luminous galactic nuclei (Frogel, Cohen, & Persson 1983). Therefore, the anomalous strength of the CO absorption confirms that the stellar output of M82 is dominated by a distinct stellar population associated with the starburst.

3.3. *Role of Hot Dust*

The presence of interstellar emission features of 3.3, 7.7, and 11.3 μm in the spectrum of M82 (e.g., Willner et al. 1977; Gillett et al. 1975) shows that the galaxy contains very hot dust particles that contribute substantially to the output longward of 3 μm. One of the goals in our spectrophotometry was to determine how significant the hot dust emission is shortward of 3 μm.

LCJG argue that the nuclear flux at 2.29 μm contains a 30% contribution from hot dust. Their suggestion is motivated by two issues. First, to reconcile the large H_2O index with output from any reasonable type of star, they require hot dust emission to dilute the CO absorption band. However, we have shown that their H_2O band strength is likely in error. Second, to reconcile the relatively small extinction inferred from $J-H$ colors with the larger extinction inferred from $H-K$, they require dust emission to contribute to the K color. As we will discuss in §3.6, this underestimate of the extinction based on short wavelength ($J-H$) colors can be easily understood if the dust is mixed with the stars rather than distributed in a foreground screen. Thus, there may be no need to invoke a contribution of hot dust to the emission at 2.2 μm.

As evidence against a hot dust component to the 2 μm emission, we consider Figure 2, which shows spectrophotometry pertaining to the nucleus and to an off-nuclear position set equal at 2.27 μm (see § 2.2). The strength of the 3.3 μm feature and the strength of the continuum at 4.9 μm both demonstrate that the hot dust component is 2 times stronger relative to the stellar output in the off-nuclear position than it is on the nucleus. Since the stellar flux is 2.1 times weaker in the off-nuclear position than on the nucleus, it follows that the hot dust emission is similar in strength at the two positions.

The strength of the stellar CO absorption is similar at both positions, as shown both by our spectrophotometry and by the spectroscopy of LCJG (their Fig. 18). Because of the higher spectral resolution of their data, we have based a calculation of the relative CO depth on the spectrum of LCJG. A comparison of the continuum between 2.25 and 2.29 μm with the CO band between 2.295 and 2.335 μm indicates that the CO index is about 0.03 larger in the off-nuclear position than it is on the nucleus, i.e., off the nucleus the CO index is about 0.24. The fact that the CO strength scales in the opposite sense from expectations if the bands were weakened by emissions from hot dust indicates that such emission does not play an important role in the 2 μm spectrum.

According to the hypothesis of LCJG, the observed CO band strength results from a stellar population with an intrinsic CO index of 0.30 which is diluted by a 30% featureless contribution by hot dust. Although individual stars can exhibit CO indices greater than 0.30, such large values are improbable for stellar populations capable of accounting for the other characteristics of M82. Starburst models (Rieke et al. 1993) show that realistic stellar populations are unlikely to have CO indices greater than 0.26, suggesting that there is little contaminaton of the CO band depth by hot dust at the nuclear position. This conclusion is even stronger at the off-nuclear position where the CO index is larger. We therefore will assume that the starlight observed in the K band along the high surface brightness regions in M82 is uncontaminated by dust emission.

Although our data apply to only two positions, the maps of Telesco et al. (1991) show that hot dust is relatively suppressed compared to cooler dust over the entire 30″ region under consideration here (see their Fig. 13). It is therefore likely that the 2 μm flux throughout this region is starlight with little contamination from hot dust emission.

3.4. *Emission-Line Spectrum*

The spectrum in Figure 3 is littered with strong and weak emission lines. In § 3.4.1 below, we discuss the [Fe II] emission lines and use them to probe the density of the emitting region. In § 3.4.2, we discuss the importance of understanding the underlying stellar continuum for measuring emission-line strengths. In § 3.4.3, we examine the molecular hydrogen emission and the excitation mechanism responsible for these lines. We defer discussion of the atomic hydrogen emission lines to § 3.5. Finally, there are many additional features in Figure 3 that could be emission lines. We have marked the strongest of these features, at $\approx$1.202, 1.206, and 1.229 μm; these features remain unidentified.

3.4.1. [Fe II] *Emission*

The [Fe II] 1.257 μm line is one of the strongest lines in the near-IR spectrum of M82. This line connects the a^4D and a^6D multiplets of Fe^+ and shares the same upper state with the (a^4D–a^4F) 1.644 μm line, which is commonly seen in starburst galaxies (Moorwood & Oliva 1988). Both of these lines have recently been detected in several Galactic and LMC supernova remnants (Oliva, Moorwood, & Danziger 1989) and might prove to be important tracers of shock activity in other galaxies (Moorwood & Oliva 1988; Graham, Wright, & Longmore 1987; Greenhouse et al. 1991).

Figure 5 shows the magnetic dipole transitions that connect a^4D and a^6D levels of Fe^+. The 1.372 μm line is outside the wavelength range of our spectrum, and the Einstein A- values of the 1.248 and 1.252 μm lines are an order of magnitude smaller than the A-values of other lines from the same upper

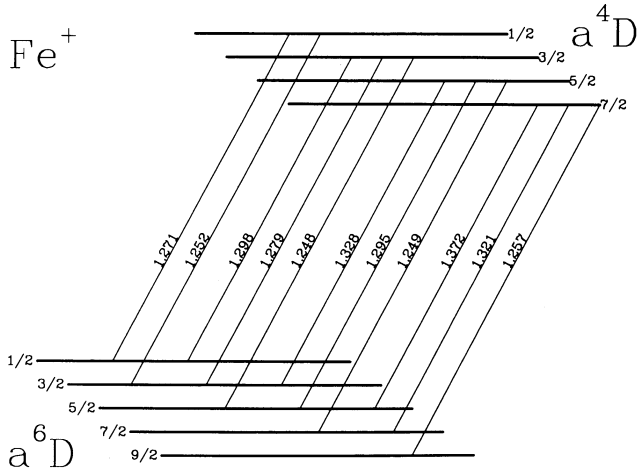

FIG. 5.—Magnetic dipole transitions between the a^4D and a^6D terms of Fe^+ (wavelengths in μm).

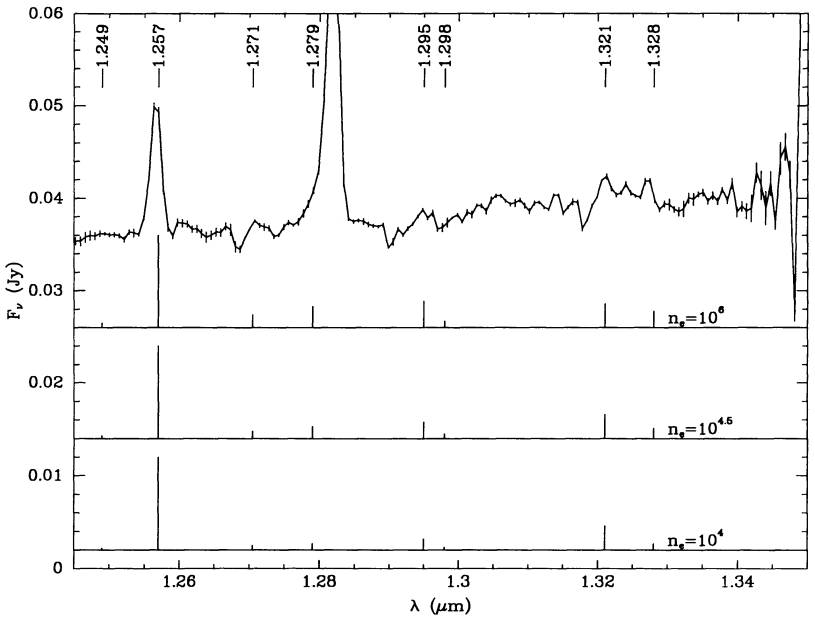

FIG. 6.—MMT spectrum of M82's nucleus, expanded to show [Fe II] emission lines. The wavelengths of the strongest lines in the a^4D–a^6D multiplet are shown above the spectrum. The predicted strengths of the lines are shown below the spectrum for several values of n_e (see text). In this plot, line height is proportional to integrated flux. The line strengths are normalized to the strength of the 1.257 μm line. Error bars are ±1 σ.

states; we ignore these lines in the following analysis. Figure 6 shows an expanded view of the MMT spectrum, covering the wavelengths of the remaining lines. LCJG detected the 1.257 and 1.321 μm lines from the nuclear position of M82; our higher resolution spectrum shows these lines as well as emission features at the positions of the 1.328, 1.279, and possibly 1.295 μm lines. The fluxes are listed in Table 1. Note that the errors given for the line fluxes do not reflect the uncertainty in the continuum level at these wavelengths (see below).

We can use these observed line ratios to probe the physical conditions of the [Fe II] emission regions. We adopt the theoretical results of Hudgins, Herter, & Joyce (1990), who considered collisional excitation of Fe^+ by electrons. They calculated the emissivities of [Fe II] 1.295, 1.279, and 1.271 μm relative to the emissivity of [Fe II] 1.257 μm. These four lines are the strongest lines from each upper state in the a^4D multiplet. Using the A-values given in Nussbaumer & Storey (1988), we compute the relative emissivities j of the remaining lines by

$$j(\lambda_{ik}) = j(\lambda_{im}) \frac{A_{ik}}{A_{im}} \frac{\lambda_{im}}{\lambda_{ik}},$$

where the i, k, and m indices refer to different energy levels of the ion. Hudgins et al. (1990) present line ratios for electron densities $n_e = 10^1$–10^6 cm^{-3} and an electron temperature $T_e = 13{,}000$ K. The resulting line ratios are very insensitive to temperature over the range $T_e = 5000$–$18{,}000$ K. Our results for densities $n_e = 10^4$, $10^{4.5}$, and 10^6 cm^{-3} are shown in Figure 6 and Table 1. Note that we have not included any extinction correction; since all of the lines are very close to each other in wavelength, the line ratios should be nearly reddening-independent.

The ratio $j(1.321)/j(1.257) = 0.26$ is constant since these two lines come from the same upper state; the ratio depends only on intrinsic properties of the Fe^+ ion. Our measured value of 0.50 may reflect the uncertainty of the placement of the 1.321 μm continuum, which we have taken to be 0.037 Jy (see Fig. 6). As we will see in § 3.4.2, the structure of the underlying stellar continuum is very complicated and may well cause us to overestimate the 1.321 μm line flux.

The similar strengths of [Fe II] 1.328 and 1.321 μm require a density $n_e \geq 10^{4.5}$ cm^{-3} to populate the $a^4D_{5/2}$ state sufficiently. A similar density is required to account for the strength of the 1.279 μm line, which arises from the $a^4D_{3/2}$ state. At a density of $n_e = 10^6$ cm^{-3}, the 1.279 and 1.328 μm line ratios match the data even better; however, at such a high density we

TABLE 1

[Fe II] EMISSION LINES[a]

TRANSITION	λ (μm)	FLUX F (10^{-17} W m^{-2})	$F_\lambda/F_{1.257}$ (measured)	$F_\lambda/F_{1.257}$ (predicted)		
				$n_e = 10^4$	$n_e = 10^{4.5}$	$n_e = 10^6$
$a^6D_{9/2}$–$a^4D_{7/2}$	1.257	5.2 ± 0.2	1.00	1.00	1.00	1.00
$a^6D_{7/2}$–$a^4D_{7/2}$	1.321	2.6 ± 0.1	0.50	0.26	0.26	0.26
$a^6D_{5/2}$–$a^4D_{5/2}$	1.295	...	...	0.12	0.18	0.29
$a^6D_{3/2}$–$a^4D_{5/2}$	1.328	2.3 ± 0.1	0.46	0.07	0.11	0.18
$a^6D_{3/2}$–$a^4D_{3/2}$	1.279	1.9 ± 0.1	0.37	0.07	0.13	0.23

[a] Measured in a 3″ beam on the nucleus; not corrected for extinction.

should easily detect the 1.295 μm line, which is only hinted at in our spectrum. We therefore take $n_e \geq 10^{4.5}$ cm^{-3} as a conservative lower limit.

The density that we determined exceeds the density $n_e < 10^{4.5}$ cm^{-3} found by LCJG using [Fe II] lines from the a^4D–a^4F multiplet; however, their result depends on an upper limit for a line that falls in a very complicated region of the spectrum (in overlapping CN and CO bands). The density we derive also exceeds that found using [Fe II] lines in Galactic supernova remnants, $n_e < 10^{4.5}$ cm^{-3} (Oliva et al. 1989).

We now compare our 1.257 μm flux with the predictions of Hollenbach & McKee (1989) assuming that shocks are responsible for the observed emission. They computed the intensity of this line as a function of shock velocity and preshock density for J-shocks in the interstellar medium. Assuming that the [Fe II] emission region fills our 3″ beam (which corresponds to a 45 pc diameter region at the distance of M82), we conclude that the shocks must be fast ($v > 60$ km s^{-1}) and that the preshock density is probably greater than 10^4 cm^{-3}. If the density is as low as 10^3 cm^{-3}, then shock velocities well in excess of 100 km s^{-1} would be required. Hollenbach & McKee (1989) do not give predictions in higher density gas than this; however, if the trend seen from $n = 10^3$–10^4 cm^{-3} continues to higher densities, then the measured line intensity can be accommodated by somewhat lower shock velocities. But, since we are underestimating the line intensity by neglecting extinction and overestimating the amount of shocked gas by assuming a filling factor of unity for the shocked gas, the density and shock velocity we derive should be treated as lower limits.

The high preshock densities inferred agree with several estimates of the densities inside molecular clouds in the center of M82. From the measurements of millimeter wavelength free-free emission, Carlstrom & Kronberg (1991) determined that the ionized gas in M82 has a larger filling factor, and that the neutral gas has likely been swept into dense clumps by supernovae and stellar winds. They derive a density $n \geq 10^5$ cm^{-3} for the neutral gas, under the assumption of pressure equilibrium. Also, the photodissociation models of Wolfire, Tielens, & Hollenbach (1990) predict cloud densities of $n \approx 5 \times 10^4$ cm^{-3}. Similarly, observations of many molecular species in M82 indicate a density $n > 10^4$ cm^{-3} (e.g., Smith et al. 1991), with about 10% of the molecular gas in the central region having $n \geq 3 \times 10^5$ cm^{-3} (Wild et al. 1992). Shocks propagating into these dense clouds might account for the [Fe II] emission we observe.

We note that the density we find here for the Fe$^+$ emitting region is much higher than the density in M82's H II regions. Measurements of far-IR fine-structure lines of [O III] and [S III] show that the H II regions have densities $n_e \approx 100$–200 cm^{-3} (Duffy et al. 1987; Houck et al. 1984). There is no contradiction here; even though the far-IR lines and the [Fe II] lines all trace ionized gas, they most likely trace different components of ionized gas. The [Fe II] lines are probably produced in the recombination zones of fast supernova remnant shocks where the gas-phase abundance of iron is high (Greenhouse et al. 1991). These shocks are relatively inefficient producers of high ionization states of oxygen and sulfur, which are easily produced in H II regions.

We stress that the value we derive for density can be only as accurate as the atomic data for Fe$^+$. Recent calculations show that the collision strengths affecting the near-IR transitions of Fe$^+$ might be factors of 2–5 higher than previously thought; thus, the densities and shock conditions derived here are very uncertain (A. Pradhan, private communication). The data we present here can be reanalyzed when the new atomic data become available.

3.4.2. *Continuum Structure*

Interpretation of weak emission features like some of the Fe$^+$ lines requires a good model for the underlying stellar continuum of the galaxy. Since red supergiants are likely to contribute significantly to the near-IR continuum of M82 (see, e.g., the models of Rieke et al. 1980, 1993), we investigate the continuum structure by plotting together in Figure 7 the spectra of M82 and two M supergiant stars: an M7 I (NGC 7419b in the notation of Blanco et al. 1955), and an M1 I (FZ Per). While the true stellar population in M82 is composed of a variety of stellar types, the M supergiant spectra are useful as templates. For example, the neutral metal absorption features at 1.267, 1.272, 1.290, 1.329, and 1.332 μm are common to the stars and the galaxy. We believe that qualitative comparisons based on the spectra are useful. For example, the relatively flat M I spectra underneath the M82 [Fe II] 1.328 μm line suggests that there is not a large contamination of that line due to the underlying stellar continuum. On the other hand, the bump at 1.3165 μm which might tentatively be identified as the ($3p\,^3P$–$4s\,^3S^o$) line of O I could instead be a continuum feature. Of course, a detailed model of M82's continuum will require higher resolution spectra of the galaxy and of a large sample of stars.

3.4.3. H_2 *Emission*

Molecular hydrogen emission has been detected in M82 by LCJG, who observed several lines in the 2 μm region of the spectrum. We report the tentative detection of several molecular hydrogen emission lines near 1.3 μm. Our spectrum contains features at the positions of the (2, 0)O(3) 1.3350, (3, 1)Q(3) 1.3237, (3, 1)Q(1) 1.3138, (4, 2)S(1) 1.3112, (2, 0)Q(1) 1.2380, (3, 1)S(1) 1.2327, (3, 1)S(3) 1.1854, and (2, 0)S(3) 1.1172 μm lines; however, comparison with M giant and supergiant spectra shows that most of these lines are likely to be contaminated by continuum structure. Confirmation of these detections will require higher resolution spectra. Note that LCJG reached a similar conclusion regarding interpretation of H_2 emission lines in the 2 μm region; they pointed out that spectra must be of high resolution to correct for continuum structure. There is a good correlation between the features we detect and the lines predicted to be relatively strong in the UV fluorescence models of Black & van Dishoeck (1987).

We measure a flux of $(1.5 \pm 0.1) \times 10^{-17}$ W m^{-2} for the 1.3138 μm line, and the other line fluxes are of the same order of magnitude; however, all of the fluxes are much more uncertain than indicated by the formal errors because of the confused continuum. We can use the 1.3138 μm line flux with the 2.122 μm flux of $(2.9 \pm 0.4) \times 10^{-17}$ W m^{-2} (LCJG) from the nuclear position to determine the excitation mechanism responsible for H_2 emission in the center of the galaxy. We define the ratio $R \equiv F(1.3138)/F(2.122)$ and find that R(measured) = 0.52, although this is only an estimate since the 2.122 μm line was measured in a slightly larger beam. Extinction to the H_2 emitting region will raise the value of R(measured) by as much as a factor of 2. The Black & van Dishoeck (1987) thermal excitation model "S2" for $T = 2000$ K predicts $R(S2) = 0.006$. Their representative model "14" for UV fluorescence pumping predicts $R(14) = 0.5$ (all the UV fluorescence models they consider predict a ratio within about 15% of the model 14 ratio). Despite the uncertainties, it is clear

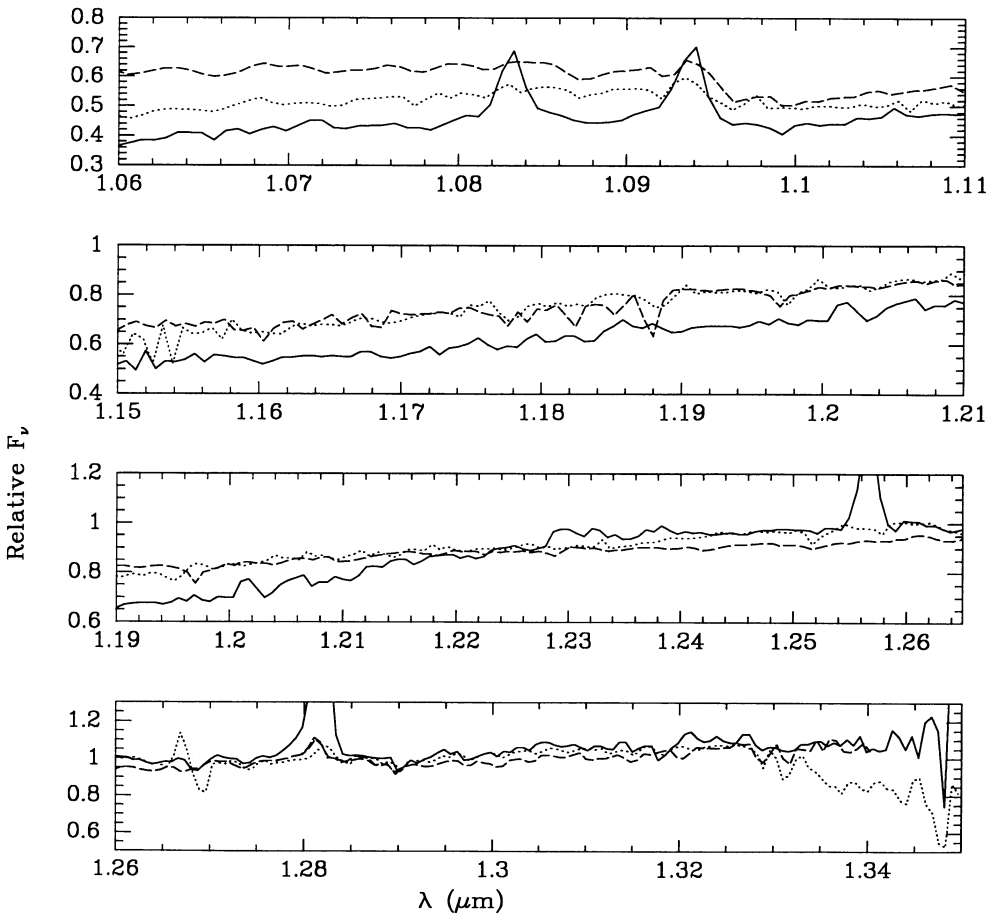

FIG. 7.—Comparison of M82 spectrum with M supergiant spectra. The solid line is M82, the dotted line is the M7 I star NGC 7419b, and the dashed line is the M1 I star FZ Per. The M I spectra have been normalized to the M82 spectrum at ≈1.285 μm. The M I bumps at the positions of the Paschen lines are due to the absorption features in the flat-field star.

that even the high temperatures considered for the thermal model cannot produce enough flux in the lines near 1.3 μm to match the observations. We conclude that UV fluorescence pumping may be responsible for a significant portion of the excitation of H_2 in M82's nucleus.

LCJG detected 2 μm H_2 emission from the nucleus of M82 but had insufficient resolution to detect unambiguously any lines near 1 μm. These authors also measured a (2, 1)S(1)/(1, 0)S(0) line ratio at an off-nuclear position. Using the Black & van Dishoeck (1987) models for H_2 excitation, they determined that far from the nucleus the ratio is more consistent with thermal excitation than with UV fluorescence. LCJG state that their measured value of this line ratio is more consistent with the value ≈0.3 predicted by the thermal models than the value ≈1 predicted by UV fluorescence models. However, some of the UV fluorescence models can give a line ratio close to 0.3. The possible similarities between fluorescently and thermally excited line ratios, combined with measurement uncertainties, can make it difficult to rule out the presence of fluorescence from the (2, 1)S(1) line strength. A combination of shorter wavelength and 2 μm lines is more diagnostic.

3.5. *Reddening Corrections for the Gas*

The large amounts of dust within M82 make reddening corrections essential for deriving the intrinsic parameters of the galaxy from near-infrared or optical observations. There are substantial disagreements on how these corrections should be made. For example, with regard to the hydrogen recombination lines, Rieke et al. (1980) conclude from measurements near the position of the 2 μm nucleus that there is highly nonuniform extinction, but the bulk of the ionized hydrogen is subject to $A_V \approx 30$. In contrast, LCJG argue that the strengths of the near-IR hydrogen recombination lines at the 2 μm nucleus are consistent with a uniform foreground screen with $A_V = 5$. However, their argument breaks down at both short and long wavelengths; they derive a visual extinction of ≈7 from the Hα/Brγ ratio and ignore Brα, which they acknowledge is far too strong to be fitted by their model.

We will show that uniform foreground screen models are incompatible with the observations. A variety of more complex models can provide a reasonable fit to the observations, such as assuming that the dust is mixed uniformly with the ionized gas, or that there is a series of absorbing screens, or that the dust is placed nonuniformly in the foreground. We consider these models below and show that there is no definitive discriminator among them; fortunately, all the models result in roughly similar estimates of many critical parameters of the starburst.

There are several caveats to keep in mind during the following discussion. Some of the line fluxes are nontrivial to determine and may contain large errors that can translate into even larger errors in the resulting estimates of A_V. Also, the extinction is patchy (see § 3.6 below) so care must be taken to choose measurements made on the same position on the galaxy.

Finally, the patchiness of the dust and the probable nonuniformity of the ionized regions warrant care in comparing measurements from different-sized beams.

For the intrinsic line fluxes we assume case B recombinations as in Osterbrock (1989; Table 4.4). We adopt the results of Puxley et al. (1989), who determined an electron temperature of $T_e \approx 5000$ K from large beam measurements of H53α and 3.3 mm free-free emission. We also take their value for the electron density of $n_e \approx 100$ cm^{-3}. For the range of hydrogen recombination lines considered here, the ratios of line flux to Brα flux are relatively insensitive to temperature and even less sensitive to density. For example, raising T_e by a factor of 2 raises the predicted line flux ratios by about 20%, which in turn raises the inferred extinctions by about 10%. Raising the density by a factor of 100 raises the predicted line ratios by less than 5%. The uncertainties in the measured line fluxes introduce at least as large an error, so we consider only the density and temperature given above. For extinction, we use the law of Cardelli, Clayton, & Mathis (1989). At Brα where this extinction law does not apply, we have used a linear interpolation of the Rieke & Lebofsky (1985) extinction law. At wavelengths where these two extinction curves overlap, their agreement is excellent.

Our hydrogen line fluxes are presented in Table 2 along with those of other authors. Also included for each measurement are the beam size and beam position relative to the nucleus. Note that our values for the Paβ flux are much smaller than LCJG value, even after appropriate beam size corrections are made (see below). Much, but not all, of the discrepancy can be accounted for by the normalization of the LCJG J-band spectrum; their continuum level does not match that predicted by the Rieke et al. (1980) J-band photometry. Some of the difference may also be attributed to the position of the beam. As shown in LCJG, there is a dip in the distribution of Brγ (and, presumably, Paβ) flux right at the position of the nucleus; thus, any measurement made slightly off center would result in a higher Paβ flux. Furthermore, if the dip results from extinction, the beam size correction may be in error.

Given the dangers of comparing hydrogen line fluxes obtained with different beam sizes, we look at the extinction puzzle in two different regimes: large beam ($\theta \geq 30''$) and small beam ($5''.8 \leq \theta \leq 11''$). In the small-beam regime, we scale the fluxes to a 6″ beam size according to the 10 μm growth curve in Rieke et al. (1980), $S_\nu \propto \theta$. Implicit in this correction is the assumption that the warm dust is a good tracer of star formation and hence of the ionized gas. For this regime, we use our 2.3 m measurements of Paβ, Paγ, and Paδ. We also choose the Simon, Simon, & Joyce (1979) position "a" beam of Brα and the O'Connell & Mangano (1978) 5″.8 Hα beam to be good matches to our 6″ data; the beam size correction factors for these lines are 0.545 and 1.03. For Brγ, the Walker et al. (1988) and the Simon et al. (1979) "a" beams are both fairly good matches to ours. However, the line fluxes do not agree with each other. We feel that the Walker et al. (1988) data are of much better quality, and their value of the flux agrees to within 10% with a beam size–corrected Brγ flux of LCJG. We therefore adopt the Walker et al. (1988) value, with the beam size correction factor of 0.769. The measured fluxes relative to Brα flux are presented in Table 3.

For the large-beam comparison, we used the Puxley et al. (1989) 41″ H53α, Willner et al. (1977) 30″ Brα, and McCarthy, Heckman, & van Breugel (1987) 90″ Hα measurements. Note that this Hα flux agrees well with the one we derived from the Young, Kleinmann, & Allen (1988) flux (see Table 2 comments). Similarly, the Brα flux agrees well with a beam size–corrected Simon et al. (1979) flux. Since the 10 μm growth curve turns over at about 30″, we assume that all of the recombination flux is contained within the central 30″; thus, no beam size corrections are required for the large-beam measurements. Table 3 shows the measured fluxes, again relative to Brα.

Also given in Table 3 are the line ratios predicted assuming a uniform foreground screen model for the obscuring dust. The observed intensity scales as $I_\nu \propto e^{-\tau_\nu}$. We show the results for $A_V = 5$, which LCJG claim is the extinction to the nucleus, and $A_V = 9$, which gives the best fit for the near-IR lines. Clearly, neither model fits the data over the entire wavelength range.

TABLE 2

HYDROGEN RECOMBINATION LINES IN M82

Line	λ (μm)	Observed Flux (10^{-16} W m^{-2})	Beam Size (″)	Position[a] (α, δ)	Source
H53α	6980	$(1.9 \pm 0.3) \times 10^{-4}$	41	(−5.7, 0)	Puxley et al. 1989
Brα	4.05	38 ± 3	11	"a" (−4.1, 1)	Simon et al. 1979
		30 ± 5	11	"b" (2.1, 5)	Simon et al. 1979
		160	30	(−4.1, 1)	Willner et al. 1977
Brγ	2.16	7.2 ± 1.7	11	"a"	Simon et al. 1979
		1.7 ± 0.4	11	"b"	Simon et al. 1979
		2.2 ± 0.2	8	(1.3, 1)	Rieke et al. 1980
		3.8 ± 0.2[b]	7.8	(1.3, 1)	Walker et al. 1988
		2.0 ± 0.04	3.8	(0, 0)	Lester et al. 1990
Paβ	1.282	1.47 ± 0.01	3	(0, 0)	This paper
		5.9 ± 0.2	6	(0, 0)	This paper
		8.0 ± 0.1	3.8	(0, 0)	Lester et al. 1990
Paγ	1.094	0.5 ± 0.1	3	(0, 0)	This paper
		1.2 ± 0.1	6	(0, 0)	This paper
Paδ	1.005	0.29 ± 0.04	6	(0, 0)	This paper
Hα	0.6563	450	90	(0, 0)	McCarthy et al. 1987
		390[c]	64	(0, 0)	Young et al. 1988
		28	5.8	(1.5, −0.7)	O'Connell & Mangano 1978

[a] Position in arcseconds relative to the nuclear position $9^h51^m43^s.6$ 69°55′00″ given in Lester et al. 1990.

[b] Derived from the Walker et al. 1988 equivalent width and Rieke et al. 1980 K photometry.

[c] Derived from the Young et al. 1988 Hα + [N II] flux of 7.7×10^{-14} W m^{-2} and the McCarthy et al. 1987 [N II]/Hα measurement of 0.5.

TABLE 3

EXTINCTION MODELS AND HYDROGEN RECOMBINATION LINE RATIOS

		Foreground Screen				
Ratio	Measured	$A_V = 5$	$A_V = 9$	$A_V = 16$ Scattering	Homogeneous Mix $A_V = 55$	2 Screen $A_V = 20$ $f = 0.15$, $g = 0.1$
Brγ/Brα	0.14[a]	0.23	0.18	0.16	0.14	0.13
Paβ/Brα	0.28[a]	0.63	0.28	0.26	0.34	0.32
Paγ/Brα	0.06[a]	0.24	0.08	0.08	0.14	0.14
Paδ/Brα	0.02[a]	0.11	0.03	0.04	0.07	0.08
Hα/Brα	1.4[a]	0.79	0.04	0.23	1.82	1.81
H53α/Brα[b]	1.2[c]	0.54	0.64	0.84	1.1	0.96
Hα/Brα	2.8[c]	0.79	0.04	0.23	1.82	1.81

[a] Small beam.
[b] Ratio × 10^6.
[c] Large beam.

Both of these foreground screen models neglect the possibility of scattering of line radiation back into the beam. As discussed by Thompson, Lebofsky, & Rieke (1978) for NGC 1068, scattering into the beam can cause the extinction to be underestimated at shorter wavelengths. To investigate the effects of scattering, we have also considered a model in which the foreground screen scatters the radiation isotropically. We have used the albedos given in Bruzual, Magris, & Calvet (1988), which are appropriate for a mix of silicates and graphite grains, but have neglected the angular dependence of the scattering. The predicted intensities in the scattering model differ from those of the nonscattering model by a factor of $e^{\tau_\nu a_\nu}$, where a_ν is the albedo. The albedos are very uncertain and small changes in the albedo can cause large changes in the predicted line ratios. Even taking the uncertainties into account, the scattering model that best fits the near-IR lines ($A_V \approx 16$, see Table 3) fails miserably at the long- and short-wavelength points, just as the nonscattering foreground screen models do.

To fit the data over the entire range of wavelengths considered here, we tested alternative models of the dust distribution. We consider (1) a "mixed" model, which describes a uniform distribution of stars mixed homogeneously with dust, and (2) a two-screen, two-source model (see Fig. 8 for notation). We neglect scattering of radiation into the beam in these models. The mixed model predicts

$$I_\nu = \frac{I_\nu(0)(1 - e^{-\tau_\nu})}{\tau_\nu}$$

and has only τ_ν as a free parameter. Of course, this is a very idealized model of a galaxy; in a real galaxy that has a concentration of stars toward its center, the mixed model might still lead to an underestimate of the total amount of light. The two-screen model predicts

$$I_\nu = \frac{I_\nu(0)(f + e^{-\tau_\nu})}{e^{g\tau_\nu}}$$

and has three free prameters, f, g, and τ_ν. In the former case, $I_\nu(0)$ refers to the line intensity in the case of zero extinction and τ_ν refers to the amount of extinction through the whole galaxy (i.e., twice the extinction to the nucleus). In the latter case, $I_\nu(0)$ refers to the line intensity from region 1 in the case of zero extinction and τ_ν represents the extinction due to the screen closest to the nucleus. Note that the two-screen formalism can also describe a single, nonuniform screen of absorbers; in this case, the parameter f is identically equal to zero, and the parameter g represents the deviation from uniform extinction. More precisely, if (x, y) are position coordinates on the surface S of absorbers each of area dA, then we can parametrize the extinction by

$$\tau_\nu(x, y) = \tau_\nu(0, 0)[1 + G(x, y)] ,$$

so that

$$e^{-g\tau_\nu} \equiv \frac{\int_S e^{-G(x,y)\tau_\nu(0,0)}\, dA}{\int_S dA} .$$

We use these formulae to determine the theoretical line ratios for different values of the extinction, f and g. The best-

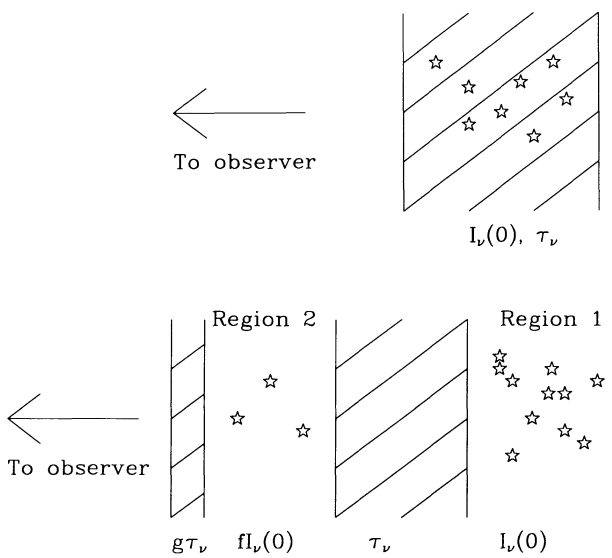

FIG. 8.—Geometry of the extinction models described in the text. *Top:* homogeneous mix of stars and dust. The parameter τ_ν is the extinction through the whole region. *Bottom:* multiple screens and sources. In the multiple screen model, region 2 has an intrinsic intensity a factor f times that of region 1, and the screen nearer the observer has an optical depth a factor g times that of the farther screen.

fitting models are summarized in Table 3. Clearly, both of these models fit better than a foreground screen model; however, we cannot distinguish between the mixed and two-screen models from these data. The real situation in M82 is most likely a combination of gas and dust mixtures and multiple screens. Since both of the best-fitting models have an extinction to the nucleus of $A_V \approx 20$–30, a combination probably would also. We conclude that the extinction is not completely understood; however, if case B recombination and a standard extinction law apply, then the extinction is probably about 27 magnitudes at V to the nucleus (or about 55 mag through the whole galaxy, assuming that the distribution of dust and stars is symmetric about the center). Our value of A_V is consistent with the extinction determined by Rieke et al. (1980), who also found that a uniform mixture of dust and stars could reproduce the near-IR observations. Puxley (1991) also shows that a foreground screen model gives a relatively poor fit to the data. For the case of a uniform mix of gas and dust, he finds an extinction of $A_V \approx 25$ through the whole galaxy. His value is somewhat smaller than ours; we believe his is an underestimate because he uses the LCJG Paβ measurement, which we think is overestimated, and because his analysis considers only a very limited wavelength range (the near-IR recombination lines).

We now compute the far-IR optical depth implied by our value $A_V \approx 55$ through the galaxy. Because the dust properties in M82 are uncertain, we have considered a range of values for the dust emissivity parameter β, where $\tau_\nu \propto \nu^\beta$. Using an extinction curve provided by J. Black (private communication) and $1.0 \leq \beta \leq 2.0$, we get $0.06 \leq \tau_{100\mu m} \leq 0.16$ and $0.003 \leq \tau_{450\mu m} \leq 0.035$. Our values are roughly consistent with the values $\tau_{100\mu m} = 0.05$ and $\tau_{450\mu m} = 0.02$ determined by Joy, Lester, & Harvey (1987) and Smith et al. (1990), respectively, from far-IR observations. The far-IR measurements would be difficult to reconcile with extinction through the galaxy of $A_V < 15$.

Using the mixed model with $A_V = 55$ through the galaxy, we can also derive the total amount of ionizing flux in the galaxy. Correcting the Willner et al. (1977) large-beam Brα flux for this amount of extinction, i.e., by a factor of 2.62, we get $F_{Br\alpha}(\text{corr}) = 4.20 \times 10^{-14}$ W m^{-2}. Using the case B, $n_e = 100$ cm^{-3} line intensity ratio $I_{H\beta}/I_{Br\alpha} = 9.62$ and recombination coefficient ratio $\alpha_B/\alpha_{H\beta}^{\text{eff}} = 8.40$, we determine that the number of Lyman continuum photons is $N_{LyC} = 1.05 \times 10^{54}$ s^{-1}. Here we have assumed a distance of 3.2 Mpc to M82 and $T_e = 5000$ K. Table 4 shows that our value of N_{LyC} is in excellent agreement with values inferred from various radio observations. Note also that the observations agree much better for an electron temperature $T_e = 5000$ K than for 10,000 K; the observations support the derivation by Puxley et al. (1989) that the temperature is low.

Finally, we investigate the effects that shocks might have on the hydrogen spectrum. Using the Hollenbach & McKee (1989) J-shock models, we find that no combination of preshock density and shock velocity that they considered can match the data. The slow shocks ($v < 40$ km s^{-1}) are inefficient producers of optical and near-IR hydrogen line emission, and they produce too little Brγ relative to Brα flux. For fast shocks ($v > 40$ km s^{-1}), the near-IR line ratios approach their recombination values, and the overall production rate of optical and near-IR hydrogen photons is boosted; however, the fast shock production of Hα is still an order of magnitude too low relative to Brα to make a foreground screen model work. Therefore, we feel that shocks do not play a significant role in producing the overall hydrogen emission-line spectrum of M82, and that the parameters that we derived based on photoionization models are justified.

3.6. *Reddening Corrections to the Stars*

The near-IR images in Figure 1 allow us to estimate the reddening to the stars. Since we have found that hot dust makes a negligible contribution to the signals in these bands, and since the intrinsic color is $H-K \approx 0.2$ for any plausible starburst stellar population, we can take the observed $H-K$ and correct it point by point to produce a reddening-corrected image of the galaxy and derive the near-IR luminosity. In this analysis we assume that the extinction for each resolution element is due to foreground dust, i.e., we assume a nonuniform foreground screen geometry overall.

Our frames were placed on the sky in a way that allowed stars and lightly obscured features in M82 to be used to adjust the scales and positions of the frames in different colors to coincide accurately. After these adjustments and a careful determination of the sky level were made, the frames were used to make a map of $H-K$ color. Local extinction values were estimated assuming an intrinsic stellar color of $H-K = 0.2$ and the reddening law of Rieke & Lebofsky (1985), which yields $A_K = 1.78E_{HK}$. The resulting extinction map is shown in Figure 9; a dereddened map of the galaxy at K is shown in Figure 10. The extinction is highly nonuniform and reaches a maximum value of $A_K \approx 1.4$, corresponding to $A_V \approx 12.5$, in a zone extending from the nucleus to the SW along the plane of the galaxy. The dereddened image of the galaxy shows a substantially enhanced nucleus and greater emission from the intense starburst region to the SW, compared with the uncorrected K image. Our map of the extinction (Fig. 9) is qualitatively similar to that of Telesco et al. (1991; their Fig. 8*a*), but we find peak extinctions of $A_K \approx 1.4$, while they find the peak extinction is only $A_K \approx 0.75$. A portion of this difference is due to the higher angular resolution of our data. However, a second difference is that our extinction measures are based on

TABLE 4

ULTRAVIOLET FLUX IN M82

REFERENCE	DATA	N_{LyC} (10^{54} s^{-1}) $T = 5000$ K	N_{LyC} (10^{54} s^{-1}) $T = 10{,}000$ K
This paper	Brα	1.05[a]	1.39
Puxley et al. 1989	H53α	1.08	1.58
Seaquist et al. 1985	Radio continuum and various recombination lines	...	0.82
Carlstrom & Kronberg 1991	3.3 mm flux	1.1	0.69

[a] Not independent of Puxley et al. 1989 value, since we used the H53α measurement to help determine extinction.

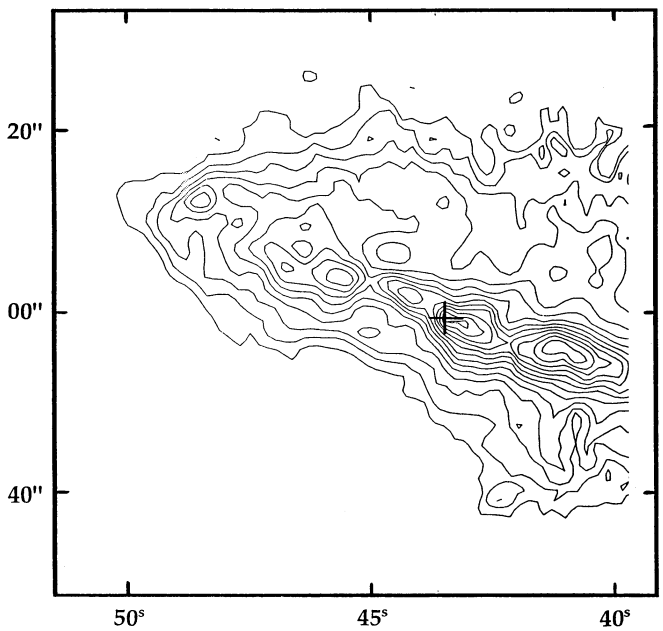

FIG. 9.—Extinction map of M82. The contour interval is 0.1 in A_K, starting at 0.2. The nuclear position at K is marked with a cross.

the $H-K$ color, whereas Telesco et al. (1991) base theirs on $J-H$ and $H-K$. *If a portion of the obscuring dust is mixed with the stars, the shorter wavelength colors, such as $J-H$, will systematically underestimate the total extinction.*

As with the gas, the extinction to the stars need not be the variable foreground screen assumed above, but could be in the form of multiple screens, a homogeneous mixture of stars and dust, or, most likely, a combination of all three geometries. The effects of different dust distributions have also been investigated by Witt, Thronson, & Capuano (1992) who reanalyzed the Telesco et al. data using a model that assumes a uniform mix of stars and dust and includes scattering. Their Figure 11 shows a maximum extinction of $A_V \gtrsim 25$ through the galaxy. Since our higher resolution images yield larger peak extinctions than the Telesco et al. data, we believe that a larger level of extinction would result if our data had been used by Witt et al. (1992). Although a difference between the extinction for the stars and the gas (for which we derived $A_V \approx 55$) might be expected, these data do not indicate a large one. Just as we found for the gas, the derived near-IR luminosity of the galaxy probably does not depend strongly on the assumed geometry of the stars and dust.

Within a 30″ aperture, the K magnitude of the image dereddened according to the nonuniform foreground screen geometry is 5.05, which corresponds at a distance of 3.2 Mpc to $M_K = -22.5$ These numbers are in close agreement with the estimates of Telesco et al. (1991), who find $m_K = 4.93$ and $M_K \approx -22.7$. Where the stars and dust are mixed, foreground screen models can yield underestimates of the total extinction and therefore of the dereddened luminosity. The value $M_K = -23$ yielded by the homogeneous mixture model of Rieke et al. (1980) is therefore fully compatible with the above estimates. Since the foreground screen results in a low estimate of overall extinction, we will adopt the value derived in that manner as an upper limit to the absolute K magnitude (i.e., it gives a lower limit to the cool stellar luminosity).

LCJG argue that the stellar flux is subject to a uniform foreground screen with $A_V \approx 5$ and that Rieke et al. (1980) overestimated the intrinsic K flux from the galaxy by a factor of 5. Part of this argument is based on their assumption that there is significant emission by hot dust at 2 μm; we have advanced new evidence against this assumption. In addition, LCJG misrepresent the model of Rieke et al. (1980) by quoting the total extinction to the nucleus in an optically thick model to compare with a foreground screen. Therefore, their comparison greatly exaggerates the difference between the two estimates. These points have been discussed by Puxley (1991), with conclusions similar to ours.

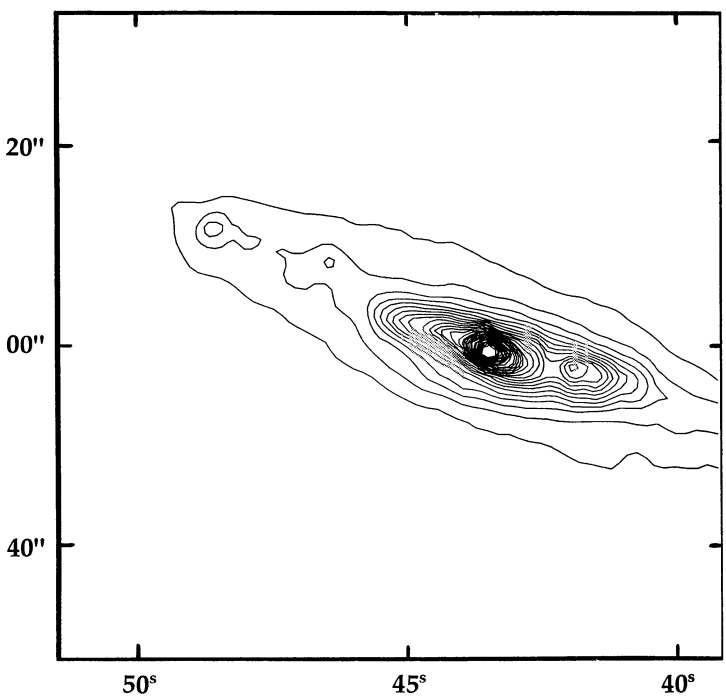

FIG. 10.—Extinction-corrected 2 μm image of M82

4. ADDITIONAL PARAMETERS

One of our goals is to reexamine carefully all the parameters relevant to starburst models such as those developed originally for M82 by Rieke et al. (1980). An accompanying paper (Rieke et al. 1993) presents a new generation of starburst models using the constraints derived in this paper. Below, we evaluate constraints that have not yet been discussed.

4.1. *Luminosity*

We need to account for three components in the luminosity of M82. The thermally reradiated far-infrared flux produces a total of $3 \times 10^{10}\ L_\odot$ (e.g., Telesco & Harper 1980). The high-resolution scans of Joy et al. (1987) show that this luminosity comes almost entirely from a 30″ diameter region. Cool stars also emit significant luminosity. Assuming a bolometric correction relative to K of +2.3 mag (typical for cool stellar populations in galactic nuclei), $M_K < -22.5$ implies a luminosity greater than $1 \times 10^{10}\ L_\odot$. Because the CO band strength is substantially stronger in M82 than in normal galactic stellar populations, this energy must be predominantly generated by

young red giants and supergiants associated with the starburst. In addition, it is likely that a significant fraction of the light from the blue stars in the galaxy escapes perpendicular to the plane. Direct evidence for this hypothesis is the pattern of polarization vectors in the filaments, which show that most of the scattered light comes from the starburst region and is bluer than the rest of the galaxy (Notni 1985). The proportion of light that escapes depends on where the obscuring dust is placed within the galaxy, which as we have seen is highly uncertain. We allow an additional $\approx 1 \times 10^{10}\ L_\odot$ for the escaping light. The total energy from the starburst is therefore greater than $5 \times 10^{10}\ L_\odot$.

4.2. *Mass*

Many differing observational techniques have been used to determine the rotation curve of M82, including measurement of: (1) optical emission and/or absorption lines (e.g., O'Connell & Mangano 1978; Saito et al. 1984; Gotz et al. 1990); (2) the [Ne II] line at 12.8 μm (Beck et al. 1978); and (3) CO lines in the mm-wave, both using interferometry (Lo et al. 1987) and high-resolution single-dish observations (Nakai et al. 1987). The latter two techniques are at wavelengths where interstellar extinction should have little effect. All the rotation velocity measurements show with excellent agreement that the dynamical mass within the starburst region (radius = 15″) is close to $6 \times 10^8\ M_\odot$. Gotz et al. (1990) propose a mass model giving

$$M(<r) = 5 \times 10^5 r^{1.33} + 4 \times 10^9 (r/2700)^2$$

(M is in $M_\odot$ and r in pc), where the first term refers to a spheroid that extends to $r = 400$ and the second term refers to a disk that extends to $r = 2700$. Within the 30″ starburst region (about 450 parsecs), this model would predict a mass of $7 \times 10^8\ M_\odot$.

We have estimated an upper limit to the mass that forms into stars in the following fashion. The overall set of events leading to the current situation was probably a close encounter with M81 about 10^8 yr ago (e.g., Solinger et al. 1977). The evolution might follow the sequence modeled by Hernquist (1989), who shows gas settling into the nucleus of a galaxy and losing its angular momentum in $\approx 10^8$ yr after an encounter. Hernquist emphasizes the role of self-gravitation of the gas in determining its dynamics and controlling when it begins star formation. By the time the mass of gas reaches the mass of the preexisting stars in the center of M82, self-gravitation in the ISM should have triggered the starburst, which has a short time scale for development compared with the gas settling time. It is therefore implausible that the total mass of ISM and stars in the burst exceeds half the dynamical mass of the nucleus. Specifically, with a maximum dynamical mass of $7 \times 10^8\ M_\odot$ and a mass currently in molecular gas of $1\text{–}2 \times 10^8\ M_\odot$ (e.g., Lo et al. 1987; Smith et al. 1990; Wild et al. 1992), an upper limit to the mass of stars that formed in the burst is $2.5 \times 10^8\ M_\odot$.

4.3. *Temperatures of Exciting Stars*

We can determine the temperatures of stars in M82's H II regions using various atomic recombination and forbidden lines. By comparing measured line ratios with ratios computed from H II region models, we derive $T_{\rm eff}$, the effective temperature of stars responsible for ionizing the gas. We adopt Rubin's (1985) spherical, equilibrium models computed for H II regions of nearly solar abundance (denoted by "K" in his tables). As discussed in § 3.5 above, we take $n_e = 100\ {\rm cm}^{-3}$. We also choose the models appropriate for a total of $N_{\rm LyC} = 10^{50}\ {\rm s}^{-1}$ ionizing photons per H II region, and assume that M82 is composed of many such regions. These models give electron temperatures of $T_e \approx 6000$ K, appropriate for the cool ionized regions in M82. We have also investigated Rubin's (1985) $N_{\rm LyC} = 10^{49}\ {\rm s}^{-1}$ models. Changing the sizes of the individual H II regions does not alter our conclusions.

Table 5 summarizes the observations and models. The third column shows the observed line ratios corrected for a total extinction of $A_V = 55$ mag through the galaxy. For the argon and neon lines, the correction is based instead on the Gillett et al. (1975) mid-IR spectrum, because the [Ar III] 8.99 μm line is superposed on the 9.7 μm silicate absorption feature. From that spectrum, we find that the correction to the 8.99 μm line flux is less than a factor of 2, relative to the other mid-IR lines. The infrared line ratios give $T_{\rm eff} \lesssim 36{,}000$ K, implying that there are few stars with masses greater than $\approx 20\ M_\odot$. The optical line ratios require $T_{\rm eff} \approx 40{,}000$ K, corresponding to stars of mass greater than $25\ M_\odot$. There is no contradiction in these results because the infrared and optical lines probe different regions of the galaxy; the optical lines sample only the foreground H II regions, whereas the infrared lines sample ionized gas throughout the galaxy. We believe that the infrared

TABLE 5

EFFECTIVE STELLAR TEMPERATURES

RATIO	MEASURED	CORRECTED	RUBIN K50 MODELS: $T_{\rm eff}$ (1000 K)				
			33	36	37	40	45
[O III] 5007 Å/[O II]3727 Å	1.2[a]	0.87	0.0067	0.10	0.23	2.7	6.3
[O III] 52 μm/Brα	6.5[b,c]	3.3	0.26	7.5	15	33	40
[Ar III] 8.99 μm/[Ar II] 6.98 μm	<0.6[c,d]	<1.2	0.20	1.3	3.7	250	480
[Ne II] 12.8 μm/[Ar III] 8.99 μm	>8[d]	>4	12	2.4	1.4	0.41	0.11
$n({\rm He}^+)/n({\rm He})$[e]	1.2[f]	1.0	0.059	0.29	0.51	0.99	1.0

[a] Peimbert & Spinrad 1970 (10″ aperture).
[b] Duffy et al. 1987 [O III] 52 μm (48″ aperture).
[c] Willner et al. 1977 Brα, [Ar II] 6.98 μm (30″ aperture).
[d] Gillett et al. 1975 [Ar III] 8.99, [Ne II] 12.8 (7″ aperture; [Ar III] scaled to 30″ for comparison with [Ar II]).
[e] Rubin does not tabulate any line ratios for helium, but does tabulate the fractional helium ionization $n({\rm He}^+)/n({\rm He})$.
[f] Determined from Peimbert & Spinrad 1970 (10″ aperture) measurement of He II(5876)/Hβ, using the formulae in that paper to get $n({\rm He}^+)/n({\rm H}^+)$, and assuming the helium abundance of the Rubin "K" models.

emission-line fluxes from the foreground H II regions are overwhelmed by the emission from the rest of the galaxy. We conclude that there are massive stars in the outer parts of the galaxy, but most of the stars with $M > 25\ M_\odot$ in the galaxy have died. This is consistent with the idea that the starburst is moving outward, with the nuclear burst being older than the main-sequence lifetimes of 25 $M_\odot$ stars, or ≈ 6.5 million yr.

Our interpretation suggests that starburst models that feature two separate episodes of star formulation should be explored. We can get a rough idea of the relative amounts of UV output from the two episodes by considering the effects of two populations of H II regions on the infrared line ratios. We assume that there is a young population of H II regions with stars as hot as 40,000 K, and an older population of H II regions with stars no hotter than 33,000 K. Using the Rubin (1985) models, we find that no more than about 25% of the UV light can come from stars hotter than 40,000 K and still satisfy the infrared observational constraints.

Finally, we consider the possible effects of shocks on the interpretation of fine structure line ratios, again using the models of Hollenbach & McKee (1989). The only fine structure line in both our analysis and the shock models is the 12.8 μm line of Ne^+. Any contribution to this line from shocked gas will raise the apparent excitation temperature slightly. The shock models show that emission in this line is maximized for fast ($v \approx 100$ km s^{-1}) shocks in dense ($n \gtrsim 10^5$ cm^{-3}) gas. However, to account for the measured flux of this line, the filling factor of the shocked, dense gas must be greater than unity in the central 500 pc diameter regon. Therefore, contamination of this line by shocked gas emission is not likely to be very significant. Although the shock models do not treat the [O III] and [Ar III] lines explicitly, we believe that contamination of these lines will be minimal because shocks are relatively inefficient producers of high-ionization lines. We cannot say quantitatively how much of the emission in each of our temperature-diagnostic lines comes from shocks. However, because the H II region assumption leads to a consistent interpretation and because some of the conditions required for shock-excited emission seem unreasonable, we believe that our results are robust.

4.4. *Metallicity*

O'Connell & Mangano (1978) deduced that the line ratios in their visible wavelength spectra are generally similar to those of H II regions with metallicity at or slightly above solar (see Peimbert 1975) but do not indicate extreme metal enhancement. Because of the high extinction, these measurements apply only to the portion of the ISM on the near side of the galaxy.

The metallicity of the ISM in the rest of the galaxy can be deduced from infrared line measures, which show roughly solar metallicity for a number of elements. Puxley et al. (1989) used previous measurements of the mid-infrared fine structure lines of argon and neon (e.g., from Willner et al. 1977), to show that the abundance of these elements are within $\pm 50\%$ of solar. Duffy et al. (1987) measured far infrared lines of oxygen and nitrogen. From the strength of the oxygen line and an assumption of solar abundances, they deduced that the H II regions in M82 require 7.5×10^{53} Lyman continuum photons s^{-1} for their excitation, only slightly lower than our estimate of 1.05×10^{54} photons s^{-1} determined from hydrogen emission lines (see § 3.5). If the entire discrepancy arises from an enhanced oxygen abundance, the oxygen is no more than 1.5 times solar abundance in the ionized gas in M82. Duffy et al. (1987) suggest that the nitrogen abundance may be significantly lower than that of oxygen, but also mention that this result depends on the nature of the ionizing field.

Recently, Gaffney & Lester (1992) have argued that the stars that dominate the 2 μm light from M82 have very high metal abundances and that any valid analyses of the population must take this situation into account. Because of the evolution time from formation on the main sequence to the red giant and supergiant phases, the stars seen at 2 μm must have formed 10 million yr ago or more, near the beginning of the starburst. If anything, the ISM should have been enriched by the stellar ejecta during the ensuing time, making it very puzzling how super metal-rich stars could have formed from an ISM of solar or lower metallicity.

To examine this question in more detail, we note that the 2 μm spectrum of M82 is expected to be dominated by supergiant stars. Fortunately, Gaffney & Lester (1992) obtained spectra of two supergiants, BS 8726 (K5 Ib) and SU Per (M3–4 Iab), whose types are representative of those expected in M82. We therefore averaged the spectra of these two stars and compared the result with the spectrum of M82 as shown in Figure 11. The figure also shows errors bars typical of the uncertainties in atmospheric corrections quoted by Gaffney & Lester (1992); since these errors vary across the spectrum, it is useful to plot typical cases individually. The close agreement between the average of the stellar spectra and that of M82 confirms the high quality of the observational data. However, in our comparison there is no significant difference at 2.227 or at 2.238 μm, both marked as "Fe," which are the two features that Gaffney & Lester (1992) assert are anomalously strong in M82. Besides the molecular hydrogen emission lines, the only possibly significant difference between the spectra is that the Na line at 2.207 μm may be slightly weak relative to the other three lines in M82. Since this line is at a wavelength where Gaffney & Lester (1992) achieved somewhat degraded corrections for atmospheric extinction (see their Fig. 2), the difference may be purely observational.

In addition to observational uncertainties, the apparent discrepancy between Figure 11 and the conclusions of Gaffney &

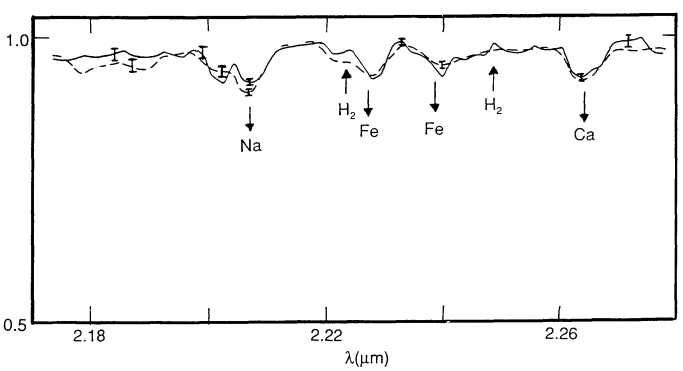

FIG. 11.—Comparison of the spectrum of M82 with normal supergiant spectra. The data are from Gaffney & Lester (1992); we have averaged their spectra of BS 8726 and SU Per (*dashed line*) for comparison with their spectrum of M82 (*solid line*). Line identifications are indicated: the H_2 lines are emission from the interstellar medium of the galaxy, and the remaining lines are absorptions in the stellar spectra. At this resolution, the lines marked "Fe" are blends that include lines from other species.

Lester (1992) could be explained if the relative stellar line strengths are a function of luminosity. A careful inspection of the stellar spectra presented by Kleinmann & Hall (1987) supports this possibility. Because of the complexity of the underlying spectra, any meaningful comparison requires that the spectra be smoothed to a resolution corresponding very closely to that achieved by Gaffney & Lester (1992). After doing so and adjusting the normalizations and slopes to achieve an accurate fit to both the 2.207 μm band of Na and the 2.263 μm band of Ca, we find that the Fe features in question are in fact stronger in μ Ceph (M2 Ia) than in χ Peg (M2 III).

It appears that the data of Gaffney & Lester (1992) can be fitted by either of two assumptions: (1) the 2 μm spectrum of M82 is dominated by red giants of extremely high metallicity; or (2) the near-IR spectrum is dominated by supergiants of roughly solar metallicity. The second explanation has the advantage of being consistent with the other evidence regarding the metallicity in M82. Further analysis of this issue will be presented in an accompanying paper (Rieke et al. 1993).

In summary, the evidence from emission-line studies of a number of elements all suggests that the present-day ISM in M82 has solar or slightly greater than solar metallicity. From this result and any plausible time scale for enrichment of the ISM during the starburst, the ISM would have been of solar or lower metallicity when the stars formed that now dominate the light in the near-IR. The stellar spectra are consistent with this conclusion so long as the near-IR is dominated by the output of red supergiants.

4.5. *Supernova Rate*

From a study of the expansion rate of the supernova remnants in M82, Bartel et al. (1987) deduce that the supernova rate is approximately 0.1 yr^{-1} in the starburst region. Kronberg & Sramek (1985) monitored the supernova remnants for period of 2.7 yr, and given the rate of fading concluded that a supernova rate of 0.2–0.3 yr^{-1} was required to maintain the appearance of the galaxy. However, since no new supernovae have appeared in the ensuing time, a rate somewhat lower than this estimate and in agreement with that of Bartel et al. would appear more appropriate (P. Kronberg, private communication); current data would suggest rates of 0.15 to 0.07 yr^{-1}.

4.6. *Age of X-Ray Wind*

Fabbiano (1988) shows that the wind detected in X-rays and blowing out from the starburst region has a maximum extent of 8 kpc and a temperature of 3×10^7 K. Although full modeling of this wind is a complex problem (see Tomisaka & Ikeuchi 1988), a lower limit for the time to reach its current extent can be derived in a simple way. The detailed models of Tomisaka & Ikeuchi (1988) show that such winds cannot break out of the plane of the galaxy until the supernova rate in the starburst significantly exceeds 0.01 yr^{-1}. Once the wind breaks out of the galaxy, its maximum expansion rate is the Maxwellian velocity of a hydrogen atom, which would require a minimum time of 10^7 yr to reach 8 kpc.

5. CONCLUSIONS

We have used a combination of visible and infrared imaging and a set of accurate telescope offsets to show the following.

i. The nucleus of M82 does not coincide with any feature that is bright in the visible.

ii. The absolute magnitude of the starburst region is $M_K < -22.5$.

New low-resolution spectrophotometry of the nucleus and an off-nuclear position in M82 indicates that:

i. The H_2O index is less than 0.06 and the CO index is $\approx$0.21 on the nucleus of the galaxy.

ii. The nuclear and off-nuclear CO bands and the K fluxes are not significantly contaminated by hot dust.

We have presented and analyzed high-resolution 1–1.35 μm spectra of the nucleus of M82, with the following results.

i. Combining our measurements of Paβ, Paγ, and Paδ with other hydrogen line fluxes available in the literature, the extinction cannot be modeled by a simple foreground screen of dust, but more complex models such as a uniform mix of gas and dust or a nonuniform screen of absorbers can provide a reasonable fit to the observations. For a uniform mixture of gas and dust, we find an extinction $A_V \approx 27$ to the nucleus.

ii. The spectrum has several lines of Fe^+, including some that have not previously been detected. We have used the relative fluxes of these lines to set a lower limit to the density of the [Fe II] emitting region, $n_e \geq 10^{4.5}$. These line fluxes are consistent with predictions for excitation due to fast shocks incident on dense gas.

iii. Several lines of molecular hydrogen are tentatively detected. If these detections are confirmed, they will indicate that UV fluorescence pumping is responsible for much of the H_2 emission. Thus they may be useful as probes of the UV radiation field inside the starburst.

These measurements and others available in the literature allow us to determine the boundary conditions for starburst models of M82. These constraints are summarized in Table 6.

We appreciate helpful discussions with J. Black, R. Kennicutt, and S. White. We thank R. Thompson and C. Walker for reading earlier versions of the paper, and Milagros Ruiz for keeping us in line. We also thank the anonymous referee for helpful commments. Assistance at the telescope was provided by J. McAfee, C. Heller, and D. Means. This work was supported by the National Science Foundation, and is based upon work supported under a National Science Foundation Graduate Fellowship.

TABLE 6

OBSERVATIONAL CONSTRAINTS ON M82 STARBURST MODELS

Date	L (10^{10} $L_\odot$)	M (10^8 $M_\odot$)	M_K	H_2O	CO	log UV	M_u ($M_\odot$)	Fe/H	SNR (yr^{-1})
1980.....	4.0	3.0	−23.0	...	...	53.3	31	...	...
1992.....	>5.0	<2.5	<−22.5	<0.06	>0.21	>54.0	[a]	≈solar	≈0.1

[a] No more than 25% of the ionizing flux form stars hotter than 40,000 K.

REFERENCES

Aaronson, M. 1977, Ph.D. thesis, Harvard Univ.
Aaronson, M., Frogel, J. A., & Persson, S. E. 1978, ApJ, 220, 442
Bartel, N., et al. 1987, ApJ, 322, 505
Beck, S. C., Lacy, J. H., Baas, F., & Townes, C. H. 1978, ApJ, 231, 28
Black, J. H., private communication
Black, J. H., & van Dishoeck, E. F. 1987, ApJ, 322, 412
Blanco, V., Nassau, J. J., Stock, J., & Wehlau, W. 1955, ApJ, 121, 637
Bruzual, G. A., Magris, G. C., & Calvet, N. 1988, ApJ, 333, 673
Campins, H., Rieke, G. H., & Lebofsky, M. J. 1985, AJ, 90, 896
Cardelli, J. A., Clayton, G. C., & Mathis, J. S. 1989, ApJ, 345, 245
Carlstrom, J. E., & Kronberg, P. P. 1991, ApJ, 366, 422
Cutri, R., private communication
Duffy, P. B., Erickson, E. F., Haas, M. R., & Houck, J. R. 1987, ApJ, 315, 68
Elias, J. H., Frogel, J. A., Matthews, K., & Neugebauer, G. 1982, AJ, 87, 1029
Fabbiano, G. 1988, ApJ, 330, 672
Frogel, J. A., Cohen, J. G., & Persson, S. E. 1983, ApJ, 275, 773
Frogel, J. A., Persson, S. E., Aaronson, M., & Matthews, K. 1978, ApJ, 220, 75
Gaffney, N. I., & Lester, D. F. 1992, preprint
Gillett, F. C., Kleinmann, D. E., Wright, E. L., & Capps, R. W. 1975, ApJ, 198, L65
Gotz, M., McKeith, C. D., Downes, D., & Greve, A. 1990, A&A, 240, 52
Graham, J. R., Wright, G. S., & Longmore, A. J. 1987, ApJ, 313, 847
Grandi, S. A. 1975, ApJ, 196, 465
Greenhouse, M. A., Woodward, C. E., Thronson, H. A., Rudy, R. J., Rossano, G. S., Erwin, P., & Puetter, R. C. 1991, ApJ, 383, 164
Hernquist, L. 1989, Nature, 340, 687
Hollenbach, D., & McKee, C. F. 1989, ApJ, 342, 306
Houck, J. R., Shure, M. A., Gull, G. A., & Herter, T. 1984, ApJ, 287, L11
Hudgins, D., Herter, T., & Joyce, R. J. 1990, ApJ, 354, L57
Joy, M., Lester, D. F., & Harvey, P. M. 1987, ApJ, 319, 314
Kleinmann, S. G., & Hall, D. N. B. 1987, ApJS, 62, 501
Kronberg, P. P., Biermann, P., & Schwab, F. R. 1985, ApJ, 291, 693
Kronberg, P. P., & Sramek, R. A. 1985, Science, 227, 4682
Lester, D. F., Carr, J. S., Joy, M., & Gaffney, N. 1990, ApJ, 352, 544 (LCJG)
Lo, K. Y., Cheung, K. W., Masson, C. R., Phillips, T. G., Scott, S. L., & Woody, D. P. 1987, ApJ, 312, 574
Lynds, C. R., & Sandage, A. R. 1963, ApJ, 137, 1005
Maloney, P., & Black, J. H. 1988, ApJ, 325, 389
McCarthy, P. J., Heckman, T., & van Breugel, W. 1987, AJ, 93, 264
Moorwood, A. F. M., & Oliva, E. 1988, A&A, 203, 278
Nakai, N., Hayashi, M., Handa, T., Sofue, Y., Hasegawa, T., & Sasaki, M. 1987, PASJ, 39, 685
Notni, P. 1985, Astron. Nach., 306, 273
Nussbaumer, H., & Storey, P. J. 1988, A&A, 193, 327
O'Connell, R. W., & Mangano, J. J. 1978, ApJ, 221, 62
Oliva, E., Moorwood, A. F. M., & Danziger, I. J. 1989, A&A, 214, 307
Osterbrock, D. E. 1989, Astrophysics in Gaseous Nebulae and Active Galactic Nuclei (Mill Valley, CA: University Science Books)
Peimbert, M. 1975, ARA&A, 13, 113
Peimbert, M., & Spinrad, H. 1970, ApJ, 160, 429
Pradhan, A., private communication
Press, W. H., Flannery, B. P., Teukolsky, S. A., & Vetterling, W. T. 1986, Numerical Recipes (New York: Cambridge Univ. Press)
Puxley, P. J. 1991, MNRAS, 249, 11P
Puxley, P. J., Brand, P. W. J. L., Moore, T. J. T., Mountain, C. M., Nakai, N., & Yamashita, T. 1989, ApJ, 345, 163
Rieke, G. H., & Lebofsky, M. J. 1985, ApJ, 288, 618
Rieke, G. H., Lebofsky, M. J., Thompson, R. I., Low, F. J., & Tokunaga, A. T. 1980, ApJ, 238, 24
Rieke, G., Loken, K., Rieke, M., & Tamblyn, P. 1993, ApJ, 412, 99
Rix, H.-W., Carleton, N. P., Rieke, G., & Rieke, M. 1990, ApJ, 363, 480
Rubin, R. H. 1985, ApJS, 57, 349
Saito, M., Sasaki, M., Kaneko, N., Nishimura, M., & Toyama, K. 1984, PASJ, 36, 305
Seaquist, E. R., Bell, M. B., & Bignell, R. C. 1985, ApJ, 294, 546
Simon, M., Simon, T., & Joyce, R. R. 1979, ApJ, 227, 64
Smith, P. A., Brand, P. W. J. L., Puxley, P. J., Mountain, C. M., & Nakai, N. 1990, MNRAS, 243, 97
Smith, P. A., Brand, P. W. J. L., Mountain, C. M., Puxley, P. J., & Nakai, N. 1991, MNRAS, 252, 6P
Solinger, A., Morrison, P., & Markert, T. 1977, ApJ, 211, 707
Telesco, C. M., Campins, H., Joy, M., Dietz, K., & Decher, R. 1991, ApJ, 369, 135
Telesco, C. M., & Harper, D. A. 1980, ApJ, 235, 392
Thompson, R. I., Lebofsky, M. J., & Rieke, G. H. 1978, ApJ, 222, L49
Tomisaka, K., & Ikeuchi, S. 1988, ApJ, 330, 695
Walker, C. E., Lebofsky, M. J., & Rieke, G. H. 1988, ApJ, 325, 687
Wild, W., Harris, A. I., Eckart, A., Genzel, R., Graf, U. U., Jackson, J. M., Russell, A. P. G., & Stutzki, J. 1992, A&A, 265, 464
Willner, S. P., Soifer, B. T., Russell, R. W., Joyce, R. R., & Gillett, F. C. 1977, ApJ, 271, L121
Witt, A. N., Thronson, H. A., Jr., & Capuano, J. M. 1992, ApJ, 393, 611
Wolfire, M. G., Tielens, A. G. G. M., & Hollenbach, D. 1990, ApJ, 358, 116
Young, J. S., Kleinmann, S. G., & Allen, L. E. 1988, ApJ, 334, L63